Journal of Cardiovascular Magnetic Resonance (2007) **9,** 327–333
Copyright © 2007 Informa Healthcare
ISSN: 1097-6647 print / 1532-429X online
DOI: 10.1080/10976640601107636

informa
healthcare

Moderated Posters Session II

Abstract Session XII: Saturday, February 3, 2007

478. EFFICIENT, ACCURATE AND ROBUST LEFT-VENTRICULAR DIASTOLIC FUNCTIONAL ANALYSIS BASED ON SHORT-AXIS CINE CARDIAC MRI

Marcel Breeuwer, PhD, Gilion Hautvast. ***Philips Medical Systems, Best, The Netherlands.***

Introduction: Congestive heart failure is increasingly becoming a problem in the elderly population and is associated with an increased morbidity and mortality. Diastolic dysfunction is an important cause of congestive heart failure. It often occurs when systolic function is still normal. Analysis of diastolic function is, therefore, becoming an important clinical application. Conventionally, diastolic functional analysis is performed on the basis of Nuclear Medicine or Echocardiography (1, 2).

Purpose: We present a method for the almost automatic determination of diastolic functional parameters from short-axis cine CMR images. We furthermore present the assessment of the accuracy and robustness of the method.

Methods: The diastolic functional parameters are derived from the volume over time curve v(t) of the left ventricle. This volume curve is obtained by first semi-automatically segmenting the left-ventricular blood pool from the cine cardiac MR images for all slices and phases using a method presented in (3) and subsequently calculating the volume per phase using the well-known Simpson's Rule.

After a spline-based temporal interpolation, the first order derivative (dv/dt) is determined and the following diastolic functional parameters are automatically estimated using this derivative: early peak filling rate, early filling volume, late (atrial) peak filling rate, late (atrial) filling volume and the time moments at which these peak rates occur. Figure 1 shows the complete set of calculated diastolic parameters.

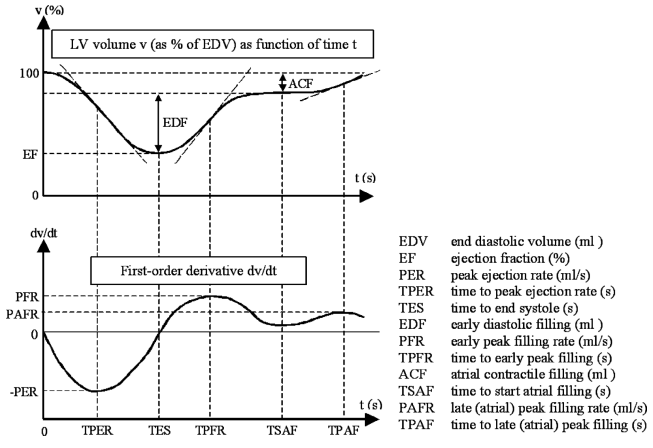

FIG. 1. Parameters derived from the volume curve v(t).

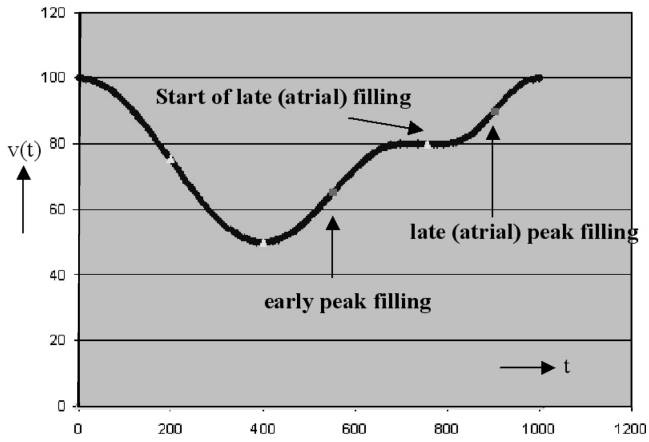

FIG. 2. Example of synthetic volume curve with detected diastolic parameters.

The accuracy of the method was assessed by applying it to synthetically generated volume curves with exactly known diastolic functional parameter values. Curves were generated with widely varying values for the number of phases in the cardiac cycle (25–50), ejection fraction (25–75%) and the ratio of the early and late (atrial) filling volumes (1.0–2.0) (Fig. 2).

The robustness of the method was evaluated by applying it to 80 cine CMR acquisitions from ischemic patients, originating from 5 different hospitals. The acquisitions had a large variety of spatial (nr. slices, voxel size) and temporal (nr. phases) resolutions. The outcome of the diastolic parameters estimation was shown visually on the volume curves, so that their correctness could be expected visually (Fig. 2).

Results: The maximum error in the diastolic functional parameters, estimated from the synthetic curves, was less than 1% for 25 phases per cardiac cycle and less than 0.5% for 50 phases, i.e., the developed algorithm can accurately derive all parameter values.

The evaluation on the 80 patient data sets showed that the values of all diastolic parameters were as expected, i.e., the developed algorithm appeared to be robust to the variation that is usually present in patient data.

The method has a high efficiency. For a 10-slice, 25-phases short-axis data set, all parameters can be derived in less than 2–4 minutes, including the semi-automatic left-ventricular blood-pool segmentation. The semi-automatic segmentation

takes over 99% of this time (on a standard 3 GHz PC with 2 GByte memory).

Conclusions: Left-ventricular diastolic functional analysis can be performed efficiently, accurately and robustly on the basis of multi-slice, multi-phase short-axis cine cardiac MR acquisitions.

REFERENCES

1. Kikkawa M, et al. Eur J Nucl Med 2001;28:593–601.
2. Dahm JB, et al. J Clin Basic Cardiol 2002;5:189–192.
3. Hautvast GLFT, et al, CARS 2005, Int. Congress Series 2005;128:351–356.

479. INITIAL EXPERIENCES ON FEASIBILITY OF ACUTE MRI FOR DIFFERENTIAL DIAGNOSIS IN CHEST PAIN UNIT PATIENTS WITH TROPONIN T RELEASE, ATYPICAL CHEST PAIN AND INCONSPICUOUS ECG CHANGES

Henning Steen, MD, Media Madadi, Stephanie Lehrke, MD, Dirk Lossnitzer, MD, Hugo A. Katus, MD, Evangelos Giannitsis, MD. ***University Heidelberg, Heidelberg, Germany.***

Introduction: MRI is a versatile non-invasive imaging method without use of radiation exposure and nephrotoxic contrast agents. Due to various different morphological and functional sequence modalities, MRI can lead to diagnosis for the entire spectrum of cardiovascular diseases.

Until now, MRI has rarely been used in collaboration with an emergency chest pain unit (CPU) for diagnosis finding in patients (pts.) with assumed acute cardiovascular events due to the perception of prolonged MRI study time and the fear of insufficient MRI physiological monitoring capabilities.

Pts. presenting with atypical chest pain, inconspicuous ECG changes but release of the cardio-specific serum marker Troponin T (TNT) are diagnostically challenging and frequently unclear or misdiagnosed. For TNT indicates cardiomyocyte necrosis due to various reasons, i.e., acute myocardial infarction (AMI), myopericarditis, pulmonary embolism (PE), aortic dissection, infiltrative diseases, cardiomyopathies, Tako-Tsubo cardiomyopathies (TT-CMP), a diagnostic method is demanded to reliably distinguish between various differential diagnosis in this pt. collective.

Purpose: We present our initial experiences and algorithm for acute MRI (AMRI) in the differential diagnosis of TNT+ pts. with atypical chest pain and inconspicuous ECG changes. We further demonstrate the feasibility to integrate the concept of AMRI into the setting of CPU pts. and demonstrate the unique capabilities of AMRI in differential diagnosis of ACS patients.

Methods: We studied 10 hemodynamically stable pts. (female = 4; mean age = 58 ± 17 ys) with TNT+ atypical chest

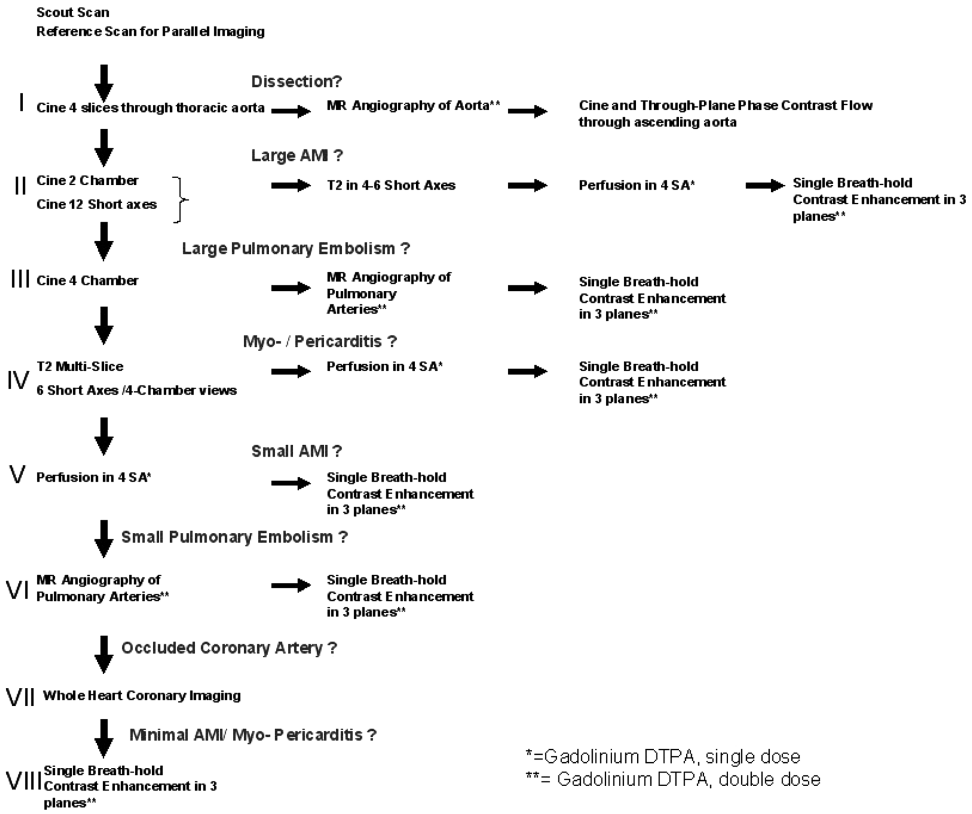

FIG. 1A. Heidelberg scan protocol of AMRI patients.

MRI Sequence	TR (ms)	TE (ms)	Reconstructed Voxel size (mm)	Flip Angle (°)	SENSE Factor	Additional Information
Cine Imaging (balanced FFE)	2.9	1.45	1.5*1.5*8	60	2.0	
T2 Imaging (Turbo-Spin)	2 RR	100	0.8*0.8*8	90	2.3	Black-blood, fat-saturation pre-pulse
Perfusion Imaging (balanced FFE)	2.8	1.4	1.5*1.5*8	50	2	
Pulmonary Angiography	2.9	1.1	0.7*0.7*2	25	2.2	CENTRA sequence, 4 dynamics
Aortic Angiography	5.3	1.6	0.8*0.8*2	20	2	CENTRA sequence, 3 dynamics
Whole Heart Coronary Imaging (3D-balanced FFE)	5.0	1.0	0.7*0.7*0.9	15	2	120 transverse slices
Scar Imaging 3D-FFE	2.9	1.0	2.0*2.0*5.0	15	2	Inversion-recovery pre-pulse (TI=200-280ms), fat saturation pre-pulse

FIG. 1B. Corresponding AMRI sequences.

pain without ECG-changes admitted to our CPU in a 1.5 Whole body MRI (ACHIEVA, Philips, The Netherlands). Pts' written informed consent was given in the CPU. For monitoring, pts' vital parameters (heart rate, blood pressure, oxygenation level, breathing curve) from CPU to MRI to CPU as well as during the MRI study, a specific monitoring table system (Philips, PhysioTrak) was used. All necessary intra-venous medications were continued using MRI-compatible infusion pumps. Contrast agent (gadolinium DTPA) was administered as shown in Fig. 1A.

The MRI protocol (Fig. 1A) was variable and consisted of up to eight steps (I-VIII). Scan parameters are shown in Fig. 1B. X-ray angiography followed the MRI scans in all pts.

Results: All pts. had no MRI contraindications and agreed to an AMRI scan which was performed successfully in all 10 pts. Mean scan time was 23 ± 22 minutes. No complications occured during transportation and AMRI study. In AMRI, five pts. revealed AMI (2 posterior, 1 lateral, 1 anterior), 2 pts. showed PE, 1 pt. had a pericarditis and 1 pt. had a TT-CMP. In one pt. no diagnosis could be found. All diagnoses were confirmed by X-ray angiography. Except for one pt. with pericarditis, all diagnoses could be confirmed by X-ray.

Conclusion: The concept of AMRI is a novel non-invasive strategy in the setting of CPU pts., which offers high diagnostic accuracy without radiation exposure and use of nephrotoxic contrast agents.

In the inhomegeneous group of TNT+ pts. from the CPU with atypical chest pain and inconspicuous ECG changes, MRI offers invaluable information for differential diagnosis, which has profound impact on pts. medical treatment as well as therapeutic strategies. Hemodynamically stable CPU pts. can be safely studied and monitored using specified AMRI protocols and cardio-dedicated monitoring systems.

480. AUTOMATED DETERMINATION OF FIRST-PASS CONTRAST ENHANCEMENT TIMING FACILITATES SEMIQUANTITATIVE AND QUANTITATIVE MYOCARDIAL PERFUSION MEASUREMENTS

Li-Yueh Hsu,[1] Daniel Mirota,[2] Christine H. Lorenz,[2] Gareth Funka-Lea,[2] Andrew E. Arai.[1] [1]***National Institutes of Health, Bethesda, MD, USA,*** [2]***Siemens Corporate Research, Princeton, NJ, USA.***

Introduction: Quantitative analysis of myocardial perfusion using first-pass contrast-enhanced magnetic resonance imaging is clinically effective but time consuming and involves user dependent steps. Non-user-dependent determination of important temporal inflection points from time-signal intensity curves could facilitate reproducible detection of the input function and other time-points necessary for measuring myocardial perfusion.

Purpose: We developed a computer program that automatically detects time-points of interest from first-pass perfusion signal intensity curves of the left-ventricle and myocardium. The computer results were compared with expert measurements of raw time-points, signal intensities, semiquantitative perfusion indices, and fully quantitative estimates of perfusion.

Methods: Rest and stress myocardial perfusion were studied using a dual-bolus protocol (0.005 and 0.1 mmol/kg of Gd-DTPA) on 8 normal subjects. Time-signal intensity curves of the left-ventricular input function (I) and myocardial enhancement (M) were generated by tracing the epicardial and endocardial borders manually. The timing of the following events was

TABLE 1

Pt.	Gender	Age (ys)	Cardiovascular risk	Sympton onset to MRI (h)	TNT admission (μg/dl)	Time to diagnosis (min)	Diagnosis	Incidents/ complications
1	f	74	HT	24	6.7	5	Posterior AMI	None
2	m	78	HT, PFH	20	0.09	45	Posterior AMI	None
3	m	79	HT, DM, HLP	14	0.09	35	Pericarditis	None
4	m	48	Smoking, PFH	10	0.47	15	Posterior AMI	None
5	f	25	None	11	0.09	10	Pulmonary Embolism	None
6	f	64	PFH	19	0.22	75	No diagnosis	None
7	m	48	HAT, HLP	24	0.19	20	Anterior AMI	None
8	f	63	None	1	0.66	15	Tako Tsubo	None
9	m	41	None	12	0.19	10	Pulmonary Embolism	None
10	m	61	HAT, PFH	24	12.22	5	Lateral AMI	None

DM = Diabetes; HAT = Hypertension; HLP = Hyperlipoproteinemia; PFH = Positive family history.

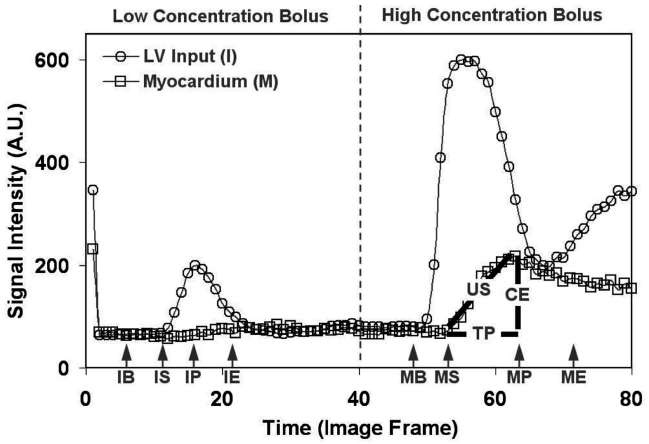

FIG. 1.

detected by a computer program for the first-pass of the contrast: 1) input function start (IS), peak (IP), and end (IE); and 2) myocardial curve start (MS), peak (MP), and end (ME). The signal intensity was measured at baseline prior to the input function (IB), prior to myocardial enhancement (MB), and peak myocardial intensity (MP) as in Figure 1. Semiquantitative perfusion indices of contrast enhancement (CE), time-to-peak enhancement (TP), and upslope (US) were calculated based on the computer and expert reader defined time-points. Fully quantitative perfusion flow measurement was also compared using a Fermi-model constrained deconvolution. The computer algorithm incorporates a piecewise cubic Hermit polynomial interpolation to increase the resolution of the time-signal intensity curves. A gamma variate function and a Gaussian/Sigmoidal mixture function were then fitted to the first-pass period of the left-ventricle and myocardium time-points respectively to smooth the signal intensity curves and to detect those timing points. Absolute errors were reported in image frame numbers and signal intensity units.

Results: Measurements of the timing of dynamic events during the first-pass perfusion showed excellent agreement between the computer and the expert reader with an average absolute error <1 image frame (Table 1). The absolute mean difference of the signal intensity averaged 3.9 ± 6.7 intensity unit which translates to $1.5 \pm 2.2\%$ of the maximum myocardium enhancement (Table 2). Semiquantitative and quantitative perfusion indices derived from the computer program correlated well with the expert measurements (Table 3). There was no significant difference between the computer and the expert generated perfusion measurements in this wide range of rest and stress perfusion measurements (all $p = NS$).

Conclusions: A computer algorithm was developed that could automatically detect all events necessary to analyze the dual-bolus first-pass perfusion protocol. Computer derived timing and signal intensity measurements replicated the results from the expert reader with minimal absolute errors. All semiquantitative and quantitative perfusion indices derived from the computer and of the expert selected time-points correlated well. Computer generated quantitative perfusion measurements can be made with one-click beyond the myocardial border tracings. The present method is also applicable for simpler protocols such as a single contrast injection.

TABLE 1
The absolute errors in image frame (RR interval)

mean ± SD	LS	LP	LE	MS	MP	ME
RR	0.9 ± 0.8	0.3 ± 0.5	0.7 ± 0.9	0.9 ± 0.7	0.7 ± 0.7	1.8 ± 1.7

TABLE 2
The absolute errors in signal intensity (% of the peak myocardium intensity)

mean ± SD	LB	MB	MP
%SI	1.9 ± 2.0	2.0 ± 3.4	0.8 ± 1.1

TABLE 3
Correlation of computer and expert generated perfusion measurements

Perfusion estimate	CE	US	TP	Flow
R	0.96	0.96	0.86	0.87

481. DELAYED-ENHANCEMENT MYOCARDIAL IMAGING IN THREE HEART BEATS IN A REAL-TIME IMAGING ENVIRONMENT

Juan M. Santos, PhD,[1] Bob S. Hu, MD,[2] John M. Pauly, PhD.[1] ***[1]Stanford University, Stanford, CA, USA, [2]Palo Alto Medical Foundation, Palo Alto, CA, USA.***

Introduction: Ischemic imaging with CVMR has revolutionized the assessment of myocardial viability. Studies have demonstrated the accuracy of the delayed-enhancement technique (1) compared to the existing gold standard of positron emission tomography. The need for accurate timing in this inversion-recovery approach using contrast in the setting of varying physiologic and pathologic kinetics has lead to inaccuracies. A number of protocol adjustments have been proposed that helped to identify and reduce these "novice" mistakes. However, because image acquisition timing cannot be determined a priori, repeated acquisitions and breath-holds are often necessary to maximize the image quality. Improvements in image acquisition have also been made in sequences, including the use of phase-sensitive inversion-recovery sequences. However, due to the inversion null, signals near the null are still not recovered using these approaches. We have developed a real-time high-resolution delayed-enhancement sequence based on our real-time architecture (2) that does not need a breath-hold, allows dynamic interactive changes of the inversion time and can step through the entire heart in less than one minute.

*Methods***:** The proposed sequence is based on a variable-density spiral trajectory that slightly undersamples high spatial

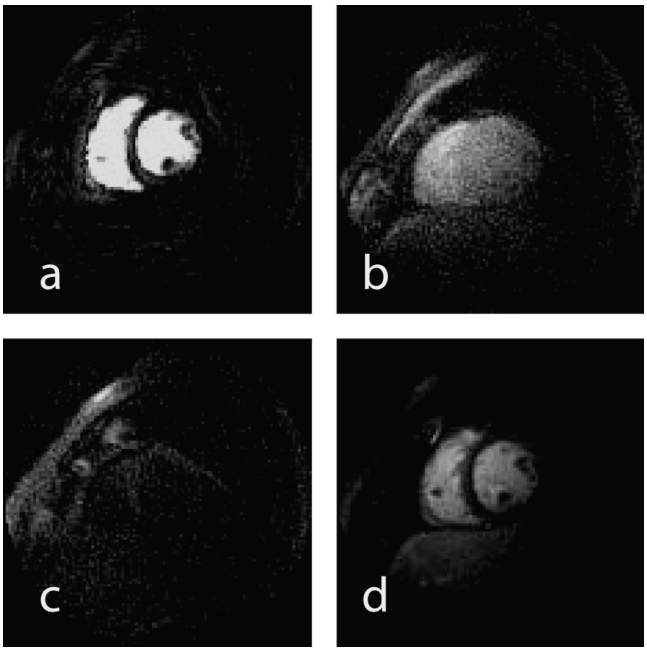

FIG. 1. Real-time delayed enhancement imaging. Total acquisition time is 3 heart beats with spatial resolution of 1.5 mm. A shows the first pass effect. B through d show the effect on the myocardium for different inversion times.

frequency components to achieve 1.5 mm resolution over a 20 cm FOV with three 16 ms interleaves. Undersampled variable-density spirals is an acquisition trajectory that can violate the sampling requirements at a benign cost of increased background noise without introducing coherent or structured aliasing artifacts (3). Because only 3 heartbeats are required to form a full image, there is no need for breath holding. In addition, the system runs in continuous acquisition mode so the image quality can be monitored for motion or breathing artifacts. The interactive capabilities of the system simplify the search for an appropriate inversion time as a simple slider can adjust TI with feedback of just a few seconds. In addition, we implemented a stepping mode that acquires multiple slices successively once a desired TI has been identified. After each cardiac trigger, a standard inversion recovery sequence is played with one of the three spiral readouts. As the real-time system allows interactively changing the acquisition waveforms, breath-held high resolution images can be acquired on demand.

Results: In the in vivo setting, the initial location, TI and FOV adjustments, and the acquisition of the entire cardiac volume can be accomplished in less than two minutes. Figures a–d show different time frames of the continuous in vivo acquisition. Figure a shows the first pass effect as the contrast bolus fills the heart chambers. Figures b–d illustrate the myocardial nulling that is obtained over a few seconds by interactively varying the inversion time.

Conclusion: Myocardial viability studies with delayed enhancement MRI are routinely done in clinical environments. Unfortunately the variable uptake and kinetics of injected contrast make the adjustment of multiple sequence parameters necessary in the course of every study. Here, we present a very fast inversion recovery technique that overcomes many of the common problems by not requiring breath-holds and by providing interactively adjustable parameters like the inversion time.

REFERENCES

1. Kim R, et al. New Eng J Med 2000;16:1445–1453.
2. Santos J, et al. IEEE EMBS Conf 2004;1048.
3. Tsai C, et al. Mag Res Med 2000;43:452–458.

482. INTEGRATED QUANTITATIVE ASSESSMENT OF SYSTOLIC AND DIASTOLIC MECHANICS OF THE HUMAN LEFT VENTRICLE: CONTINUED CIRCUMFERENTIAL SHORTENING DURING UNTWISTING

Iris K. Rüssel, MSc,[1] Marco J. W. Götte, MD, PhD,[1] Jaco J. M. Zwanenburg, PhD,[2] Sandra R. R. Tecelao, MSc,[3] Albert C. van Rossum, MD, PhD,[1] Tim Marcus, PhD.[1] [1] *VU University Medical Center, Amsterdam, The Netherlands,* [2] *Image Sciences Center, Utrecht University, Utrecht, The Netherlands,* [3] *Institute of Biophysics and Biomedical Engineering, University of Lisbon, Lisbon, Portugal.*

Introduction: Several studies have demonstrated a relation between left ventricular (LV) circumferential strain and torsion (1, 2). However, until now, systolic and diastolic strain-torsion data have not been combined, while data on human subjects is scarce and often with low temporal resolution (TR). Therefore, in this study we analyzed circumferential strain and torsion over both systole and diastole in healthy volunteers with high TR.

Methods: In 13 healthy subjects (41.6 ± 11.5 years, 3 female) the LV was imaged in 5 equidistant short-axis slices from base to apex with high TR (14 ms) CSPAMM tagging MRI (3). The timings of aortic valve closure (AVC) and mitral valve opening (MVO) were determined from a high TR (14 ms) long-axis cine. The motion of the myocardium in the basal and apical slices was automatically tracked, using the extended HARP method (4).

For every correctly tracked point in the myocardium, the rotation around the moving centroid was calculated. Counter-clockwise rotation as seen from apex to base was considered positive. The difference in rotation relative to the first time-frame between apex and base was normalized to the size of the heart, such that torsion can be interpreted as the mid-myocardial circumferential-longitudinal shear angle. Circumferential strain was calculated from the mean of all slices using the HARP method (5).

Correlations were calculated by linear regression. Timings were corrected for RR interval duration and compared by paired Student's t-test. P-values below 0.05 were considered significant.

Results: The time to peak torsion did not significantly differ from the time of AVC ($p = 0.67$) and therefore coincides with

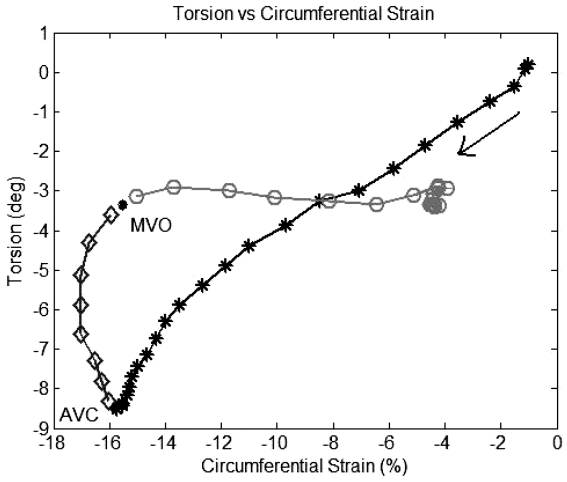

FIG. 1. Torsion plotted versus circumferential strain for a healthy volunteer. A linear relationship during systole (blue line) (1), and the occurrence of rapid untwisting before lengthening (magenta and green lines) (2) are visible.

the beginning of rapid untwisting of the LV. Circumferential shortening proceeded after the onset of untwisting in all subjects. After peak torsion, circumferential shortening increased further by 2.5% ± 0.7% ($p < 0.0001$), and reached its peak 32 ms ± 14 ms later ($p < 0.0001$) (Fig. 1).

Moreover, the correlation between the time to peak torsion and the time to peak strain was very strong ($p < 0.0001$, $r = 0.95$) (Fig. 2).

Discussion and Conclusion: The process of rapid untwisting starts directly after AVC (end ejection) and lasts until MVO (beginning of LV filling). A substantial amount of circumferential shortening was observed during this period in all subjects, which is therefore likely to be continued active myocyte contraction. Accordingly, these results are in line with recent findings about untwisting being an active myocyte shortening process (6), caused by contraction of the ascending apical myofibers. However, this was only demonstrated in animals. To investigate to what extent our findings support the ventricular myocardial band concept (7), the relation between strain and torsion must be calculated on a regional basis in future research. The proposed method allows for an integrated evaluation of strain and torsion during systole and diastole in humans. This may be of help to improve the understanding of the relation between contraction and relaxation of the myocardium.

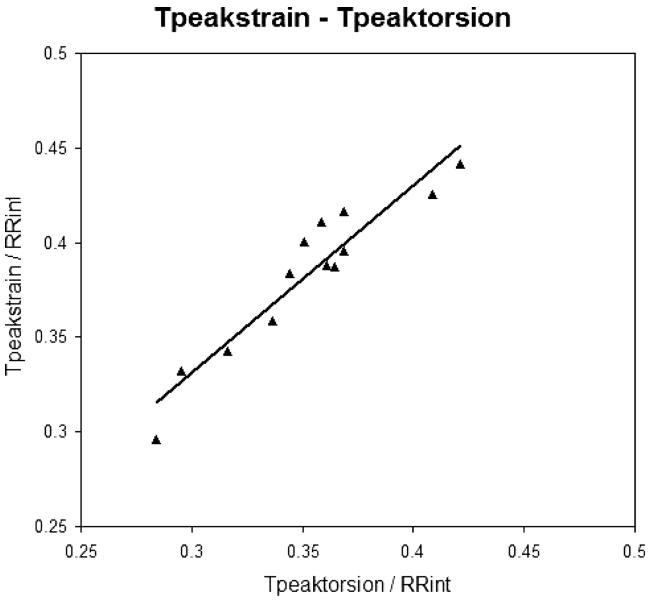

FIG. 2. Correlation between time to peak torsion and time to peak strain.

REFERENCES

1. Aelen, FWL et al. J Biomech 1997;30:207–212.
2. Rademakers FE, et al. Circ 1992;85:1572–1581.
3. Zwanenburg JJM, et al. Magn Res Med 2003;49:722–730.
4. Tecelao SRR, et al. J Magn Res Im 2006;23:682–690.
5. Kuijer JPA, et al. Magn Res Med 2001;46:993–999.
6. Buckberg GD, et al. Eur J Cardiothorac Surg 2006;29S:S98–S106.
7. Torrent-Guasp F, et al. Eur J Cardiothorac Surg 2005;27:191–201.

483. IMPROVED INTER-OBSERVER VARIABILITY OF SHORT AXIS LV VOLUMETRY BY LONG AXIS CROSS-REFERENCES

Lucia K. C. Ma,[1] Michael L. C. Ma,[1] Andreas Kumar, MD,[1] Myra Cocker,[1] Jordin D. Green, PhD,[2] Matthias G. Friedrich, MD.[1] [1]***Stephenson CMR Centre, University of Calgary, Calgary, AB, Canada,*** [2]***Siemens Medical Solutions, Calgary, AB, Canada.***

Introduction: The assessment of systolic left ventricle (LV) function is traditionally performed using a 3-D stack of multiple short axis cine images (SAX); however, partial volume effects at the base may cause inaccuracies because the short axis view does not show whether the slice contains atrial or ventricular blood.

We assessed, whether a corrected SAX (corSAX) using corresponding long axis views for assessing positioning of the basal short axis slice approach yielded improved inter-observer variability.

Materials and Methods: We assessed 46 patients (29 male, 47 ± 18) referred for a functional evaluation on a 1.5 T system (Avanto, Siemens Medical Solutions). Standard SSFP cine sequences were used for all approaches, with a slice thickness of 8 mm and a 2 mm gap for the SAX. SAX was performed as multiple short axes across the entire left ventricle in an imaging plane perpendicular to the long axis of the LV. The basal slice was included if more than fifty percent of the circumference contained myocardial tissue. CorSAX were obtained after correction of the SAX based on long axis cross-reference.

Endocardial and epicardial contours were drawn for the LV at end systole and end diastole in each data set using a clinically validated software (cmr[42], Circle International, Calgary,

Canada). In SAX analysis, papillary muscles and trabeculations were included into myocardial tissue. The time needed to complete assessments was recorded.

End-systolic and end-diastolic volume, stroke volume, ejection fraction, and LV mass were assessed by two independent observers. Inter-observer variability was measured by calculating the correlation coefficient and the mean difference of the pair observations using a statistics software (Microsoft Excel for Mac, Microsoft Corporation, USA).

Results: There was a good correlation between SAX and corSAX results. Interosberver variability however differed. Intraobserver correlation coefficients for SAX, and corSAX are shown in Table 1 along with the mean difference, standard deviation and p value.

Time of evaluation for both SAX and corSAX did not differ.

TABLE 1
Inter-observer variability correlation coefficients

	corSAX		SAX		
	r^2	Mean diff	r^2	Mean Diff	p value
EDV	0.96	13.54 ± 11.59	0.97	31.86 ± 22.57	< 0.01
ESV	0.99	7.549 ± 10.89	0.99	12.12 ± 15.55	< 0.05
EF	0.99	0.3272 ± 4.195	0.89	0.5463 ± 5.387	0.3
ES Mass	0.93	30.75 ± 28.31	0.99	31.26 ± 18.52	<0.01

Conclusion: For analyzing LV volumes and function in short axis stacks, using a long axis cross-reference reduces inter-observer variability for end-systolic volumes and ejection fraction. Long axis views should be used routinely to determine the position of the most basal short axis slice.